IOP Publishing Journal of Physics: Condensed Matter
J. Phys.: Condens. Matter **27** (2015) 085003 (8pp) doi:10.1088/0953-8984/27/8/085003

The LVV Auger line shape of sulfur on copper studied by Auger photoelectron coincidence spectroscopy

G Di Filippo[1,8], M I Trioni[2], G Fratesi[3,4], F O Schumann[5], Z Wei[5], C H Li[5], L Behnke[5], S Patil[5], J Kirschner[5,6] and G Stefani[7]

[1] Scuola dottorale in Matematica e Fisica, Università di Roma Tre, via della Vasca Navale 84, I-00146 Rome, Italy
[2] CNR—National Research Council of Italy, ISTM, Via Golgi 19, I-20133 Milano, Italy
[3] ETSF, CNISM and Dipartimento di Scienza dei Materiali, Università degli Studi di Milano Bicocca, Via Cozzi 55, I-20125 Milano, Italy
[4] Dipartimento di Fisica, Università degli Studi di Milano, Via Celoria 16, I-20133 Milano, Italy
[5] Max-Planck-Institut für Mikrostrukturphysik, Weinberg 2, D-06120 Halle, Germany
[6] Institut für Physik, Martin-Luther-Universität Halle-Wittenberg, D-06099 Halle, Germany
[7] Dipartimento di Scienze and CNISM, Università di Roma Tre, via della Vasca Navale 84, I-00146 Rome, Italy

E-mail: filippo@mpi-halle.mpg.de

Received 25 September 2014, revised 19 December 2014
Accepted for publication 6 January 2015
Published 4 February 2015

Abstract

We have studied the line shapes of Cu(0 0 1)-$p(2 \times 2)$S L_2VV and L_3VV Auger decay by means of Auger photoelectron coincidence spectroscopy. Measuring the LVV Auger spectrum in coincidence with S $2p_{1/2}$ and $2p_{3/2}$ photoelectrons respectively, we have been able to separate the two overlapping Auger spectra and determine their intrinsic line shapes. The two Auger transitions, though shifted in energy, display an identical line shape whose main features can be qualitatively understood considering a single particle approximation but are better described within a Cini-Sawatzky (CS) approach. Comparison between the experimental and the CS calculated spectra confirms that a substantial part of the Auger lines (∼20%) can be ascribed to decay events accompanied by the excitation of one additional electron–hole pair in the valence band. For the first time, the locality of the Auger process combined with the surface sensitivity of the APECS technique and its ability to separate overlapping structures are used to study Auger transitions taking place at the the surface states of a S/noble-metal interface.

Keywords: sulfur, APECS, photoemission, Auger

(Some figures may appear in colour only in the online journal)

1. Introduction

The line shape of core-valence–valence (CVV) Auger spectra has attracted the attention of scientists since the early 1950s [1]. This is because the Auger process is strongly influenced by the correlations among the electrons of a system and carries unique information on their strength. The effects of electronic interactions can be observed in both the transition energies and line shape of the Auger process [2], as illustrated by the Cini-Sawatzky (CS) theory [3, 4]. The CS model describes the continuous transformation of the Auger line shape from a simple band-like self-convolution of the valence band density of states (SCDOS), to an atomic-like one as a function of the ratio U/W. The valence band width is given by W while U corresponds to the Coulomb energy cost to place two electrons on the same atomic site [5, 6]. It is a central parameter in many theoretical descriptions beyond the mean field approximation,

[8] Present address: Max-Planck-Institut für Mikrostrukturphysik, Weinberg 2, D-06120 Halle, Germany.

for example, LDA + U approaches [7–9] or dynamical mean field theory [10]. The theoretical determination of U in the valence band of solids is made extremely difficult by the fact that its value is reduced from the atomic one by a variety of screening and relaxation processes [11, 12]. Therefore the experimental determination of the two-hole correlation energy is of fundamental interest in modern physics. The two-hole correlation energy is by definition the difference in energy between the two-particle state and the two single-particle ones. This can be easily identified for strongly correlated systems ($U/W \gg 1$), where the interaction between the final-state holes leads to the appearance of sharp atomic-like transitions [2, 13]. The CS Hamiltonian generalizes that concept, making it applicable to band-like valence and Auger spectra. So the comparison between the measured two-particle spectrum and the self-convoluted single-particle ones is the way to determine U as close as possible to its definition and such an approach has often been adopted in the literature to evaluate U from experimental data [14–20].

A major advance for the analysis of Auger transitions was the development of Auger-photoelectron coincidence spectroscopy (APECS), in which one detects Auger and photoelectrons that are correlated in time and hence originate from the same ionization event [21, 22]. In this way one is able to select events associated to the decay of a specific single hole state and this is an essential aspect when the spin–orbit splitting of a core-hole multiplet is smaller than the Auger profile width, so that different decays overlap. From the pioneering experiment performed by Haak *et al* [21], which demonstrated the feasibility of APECS, the experimental advances, particularly the development of multichannel electron detectors and the advent of energy tunable synchrotron radiation sources stimulated a renewed interest in the study of Auger line shapes of solid [23–25] and molecular targets [26–28]. A number of experiments conducted to date have shown that APECS has the ability to: isolate individual sites in a solid and probe their local electronic structure [29–31], separate overlapping spectral features [32–34], probe electronic structure with extremely high surface sensitivity [35–37].

As a consequence of these properties, See *et al* [38] have observed an enhanced sensitivity of APECS to oxygen vacancies on a TiO_2 surface. This suggested the possibility of making use of this technique to investigate the interaction of atomic and molecular adsorbates with surfaces [39].

In this paper we have measured the L_2VV and L_3VV Auger spectra of sulfur adsorbed on Cu(0 0 1) in the $p(2 \times 2)$ reconstruction. The spin–orbit splitting of S $2p$ levels is about 1.1 eV while the corresponding Auger lines span over 12 eV, thus they overlap significantly. Measuring the LVV Auger electron distribution in coincidence with $2p_{1/2}$ and $2p_{3/2}$ photoelectrons we have been able to separate the two overlapping spectra and obtain their intrinsic line shapes. The coincidence results reveal that, even though the main features of the measured spectra can be explained by the SCDOS, better refinements are obtained if a hole–hole correlation energy of $U = 0.3 \pm 0.1$ eV is taken into account. Still, a pronounced mismatch between the experimental and CS theory-based calculated spectra is observed at low kinetic energy. These extra features carry nearly 20% of the spectral weight and are associated to CVV Auger events that leave the valence band in a state that contains more than two holes.

2. Methods

All the data reported here were acquired at the beamline UE56/2-PGM2 at the storage ring BESSY II in Berlin [40]. The coincidence spectrometer, described in detail elsewhere [41, 42], consists of two hemispherical analyzers equipped with micro channel plates detectors (MCPs) and a time logic unit used to record the kinetic energy and the arrival time at the detectors of each emitted electron. In this way it is possible to record the distribution of the differences between the arrival times of two electrons ('time spectrum' of the experiment). Subtracting the coincidences due to uncorrelated events, which give rise to a continuous background whose modulation results from the time structure of the storage ring fill pattern [24], from the peak due to detection of particles generated in the same physical events [43], one is able to determine the number of true coincidences and to obtain a 2D coincidence spectrum in which the number of correlated electron pairs is reported as a function of the emitted electrons energies.

The experimental setup is schematically illustrated in figure 1. The light produced by the UE56 planar undulator impinges on the sample with a grazing angle of 10°. The optical axis of the left (vertical) and of the right (horizontal) analyzer are mutually perpendicular and they both lie in the plane perpendicular to the incident light direction, with the right analyzer aligned to the [1 0 0] direction of the sample surface. Each analyzer accepts an angle of about ±15° around the electron optical axis. The sample was tilted in such a way that the angle between the normal to the surface and the two analyzers' optical axis was equal to 45°. The two spectrometers were set to detect kinetic energies in a range of 27 eV around a mean kinetic energy of 145 eV, with a resolution of 0.8 eV.

The incident radiation energy was $h\nu = 301$ eV; at this photon energy the analyzers cover, within their energy window, both the photoelectrons coming from sulfur $2p$ levels (132 eV $\leqslant E_k \leqslant$ 136 eV) and Auger electrons from $L_{23}VV$ Auger decay (140 eV $\leqslant E_k \leqslant$ 155 eV). The energy calibration of the two analyzers was performed in a two step approach. First of all, the linearity of the spectrometers' energy scale was tested by exciting the sample with an electron beam of known accelerating voltage and by detecting the electrons elastically scattered from the surface. In order to verify that the peak position on the spectrometers moved linearly with the kinetic energy, the energy of the incident beam was moved by 1 eV steps throughout the whole energy window accepted by the analyzers. Finally, the absolute energy scale was fixed by comparing the measured kinetic energy of the S $2p_{1/2}$ and $2p_{3/2}$ photoemission peaks with the binding energies found in the literature [44–46].

The Cu(0 0 1) surface was cleaned following standard procedures consisting of Ar^+ sputtering and annealing cycles. The S/Cu(0 0 1) film was prepared by exposing the substrate

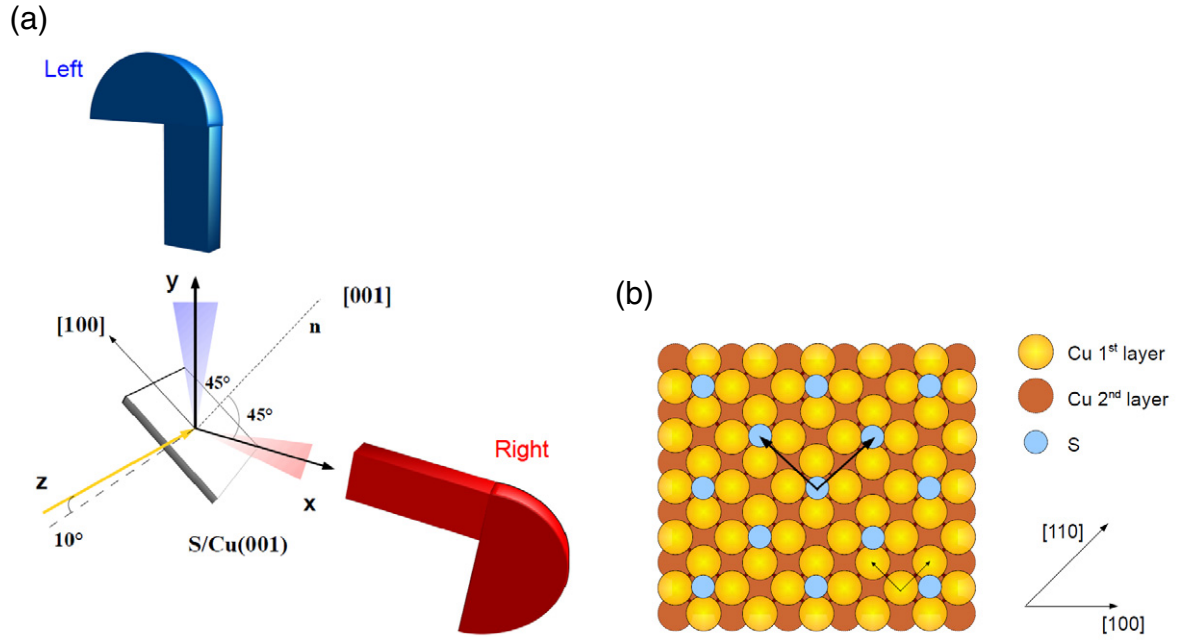

Figure 1. (*a*) Schematic of the coincidence setup to detect Auger electrons and photoelectrons. (*b*) Schematic top view of Cu(0 0 1)-$p(2 \times 2)$S surface reconstruction. The small circles represent the S adatoms, the big circles the Cu atoms in first (light orange) and second (dark orange) layer. Thin and thick arrows represent Cu(0 0 1) and S/Cu(0 0 1) surface lattice vectors, respectively.

to 20 L of H_2S gas at room temperature as set out in the literature [47]. After dosing, the sample was annealed at 300 °C. This sample gave a $p(2 \times 2)$ LEED pattern similar to that reported in previous studies [47–50]. This corresponds to a S coverage of 0.25 monolayers.

Numerical simulations within the density-functional theory (DFT) were performed to determine the electronic properties of the system with the Perdew–Burke–Ernzerhof (PBE) functional for exchange and correlation [51]. We have considered a 9-layer thick Cu slab with S adsorbed on one side and relaxed its coordinate together with 3 Cu layers underneath in a $p(2 \times 2)$ structure as depicted in figure 1(*b*). The plane-wave, ultrasoft pseudopotential method was used as implemented in the QUANTUMESPRESSO simulation package [52]. Our results for the density of states (DOS) are analogous to those reported in the literature with full potentials and the local density approximation [53].

The interaction between the two holes in the valence shell was treated by the CS theory [3, 4]. It allows for a formal solution of a many-body Hamiltonian in the case of closed bands, but its results will be tentatively applied here also in the case of S/Cu(0 0 1) whose p states are not completely filled and which would in principle require the evaluation of higher-order propagators [54, 55]. In practice, from the non-interacting DOS of the two particles, which is evaluated as the convolution of the single-particle (DFT) ones, one constructs the non-interacting Green function G_0. Eventually, a Dyson equation with kernel U allows for determining the interacting Green function G:

$$G(E) = G_0(E) + G_0(E)UG(E). \quad (1)$$

The resulting two-particle DOS can be directly compared to Auger measurements under the assumption that matrix elements are constant across the spectrum. While for atomic-like spectra the full dependence of U on the specific two-particle states has to be taken into account to correctly reproduce the observed multiplets [2], here a scalar form of (1) will be used with the DFT DOS averaged over the quantum numbers and with an effective value of U to be determined phenomenologically.

3. Results

3.1. Photoemission spectrum

The kinetic energy distribution of photoemitted electrons from Cu(0 0 1)-$p(2 \times 2)$S $2p$ levels was recorded by both spectrometers. The spectrum acquired by the right analyzer is shown in figure 2. The photoemission measurement was performed in order to verify the cleanness of the adsorbate-substrate system and to determine the kinetic energies of electrons emitted from S $2p$ levels, that will be used in the coincidence experiment. To this end, the measured spectrum was fitted by means of two Voigt profiles, accounting for $2p_{3/2}$ and $2p_{1/2}$ photoemission peaks, superimposed on a polynomial background which takes into account the inelastic scattering and the analyzer's transmission effects. The results of the fitting procedure are listed in table 1. The Gaussian full-width at half maximum was forced to be the same for both peaks and equal to the experimental resolution $W_G = 0.8$ eV, while the Lorentzian full-width at half maximum W_L, which is essentially due to the core-hole lifetime was left as a free parameter. The obtained parameters are similar for both analyzers; the kinetic energies of the spin–orbit doublet are $E_k(2p_{3/2}) = 134.85$ eV and $E_k(2p_{1/2}) = 133.7$ eV, with a spin–orbit splitting for S $2p$ levels of $\Delta E_{SO} = 1.15 \pm 0.03$ eV, consistent with previous

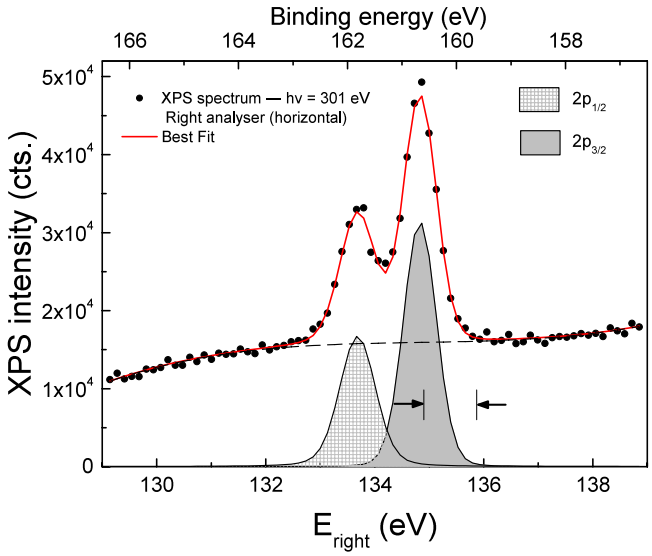

Figure 2. Cu(0 0 1)-$p(2 \times 2)$S $2p$ photoemission spectrum (black points) with $h\nu = 301$ eV; the curve was fitted with two Voigt profiles accounting for $2p_{3/2}$ (full area) and $2p_{1/2}$ photoelectrons (shaded area) and a polynomial background (dashed line). The arrows indicate the energy window for APECS measurement of the L_3VV line.

results [56]. Results show a Lorentzian width $W_L < 0.1$ eV for the L_3 peak, while the one of the L_2 is larger, $0.1\,\text{eV} \leqslant W_L \leqslant 0.2$ eV. This means that the $2p_{3/2}$ core-hole lifetime is longer than the $2p_{1/2}$ one showing that there could be additional decay channels for the latter level with respect to the former one, for example radiative decays. Given the small spin–orbit splitting, the L_2VV and L_3VV spectra overlap significantly, forbidding a detailed analysis of the LVV lineshape on the basis of conventional (single) Auger spectra.

3.2. Coincidence spectrum

Figure 3 represents the 2D distribution of correlated electron pairs, i.e. the number of coincident electrons as a function of their energies (E_{left}, E_{right}). The 2D spectrum shows four very intense features superimposed on a very low background. These high intensity features are characterized by the fact that one of the two detected electrons' energy is included in a small region around the measured S $2p$ photoelectrons' kinetic energies, while the energy of the other one spans almost the whole detected energy region. This means that a broad Auger spectrum is correlated to each of the two photoemission peaks.

An analogous 2D spectrum has already been measured by van Riessen *et al* [41] for Cu $M_{45}VV$ Auger decay. The authors observed a continuous energy sharing between photo- and Auger electron, with the emitted electron-pair characterized by a constant sum energy. This enlightened the single-step nature of the super Coster–Kronig transition, with the emitted pair acting like one entity [57–59]. In contrast, no evidence of electron energy sharing is observed in S $L_{23}VV$ transitions. These events would result in a characteristic diagonal feature ($E_{\text{left}} + E_{\text{right}} = \text{const.}$) in the 2D distribution which is not visible in figure 3. Thus, the considered Auger decay acts as a two-step process, where the photoemission and Auger transition can be considered as independent, sequential processes. This model excludes a continuous energy sharing between the emitted electrons. The difference between Cu and S cases could be due to the fact that the lifetime of the Cu $3p$ core levels involved in the decay is much shorter than the one of the S $2p$ core levels, as can be seen from previous single photoemission studies [60]. In the case of sulfur the single core hole state is long-lived enough to be considered a stationary state and the Auger decay can be described as a two-step process.

3.3. L_3VV spectrum

One of the main advantages of the coincidence spectrometer used lies in the fact that we can measure coincidences at different electron energies in parallel, remarkably reducing the acquisition time. Once the 2D distribution is acquired one can perform cuts at given energies and isolate specific coincidence events.

In our case two different cuts were performed in order to obtain the APECS spectra for the L_3VV ($2p_{3/2}$-valence–valence) and L_2VV ($2p_{1/2}$-valence–valence) Auger decays. A first spectrum, L_3VV, was built by reporting the number of coincidences in the region $134.9\,\text{eV} \leqslant E_{\text{left}} \leqslant 135.9\,\text{eV}$ as a function of the energy of the right analyzer, E_{right}. This cut was chosen in order to avoid contamination from the $2p_{1/2}$ decay. Indeed, the vertical analyzer is tuned on the high kinetic energy side of the $2p_{3/2}$ photoemission peak (see arrows in figure 2), while the horizontal analyzer captures the whole Auger spectrum.

A second spectrum, L_2VV, was built in a similar way only changing the energy of the fixed energy analyzer. In this case the left analyzer is tuned on the low kinetic energy side of the $2p_{1/2}$ photoemission peak, i.e. the selected events are located in the region $132.7\,\text{eV} \leqslant E_{\text{left}} \leqslant 133.7\,\text{eV}$. Analogous spectra have been constructed exchanging the role of the two analyzers, i.e. the right one is fixed on the $2p_{3/2}$ ($2p_{1/2}$) photoelectron while the left analyzer spans all over the L_3VV (L_2VV) Auger spectrum.

We now present in detail the results for the L_3VV Auger line measured in coincidence, shown in figure 4. The black dots in panel (a) represent the Auger spectrum recorded by the left analyzer when the right analyzer is fixed on the $2p_{3/2}$ photoelectron, while the open circles represent the same spectrum measured when the role of the analyzers is exchanged. The curves were normalized to the same maximum intensity, in order to account for the different efficiency of the detectors. The point by point difference of the measured line shapes, panel (b), shows values randomly distributed around zero, as expected. This confirms that the two independent measurements of the Auger line shape are equal within the obtained statistics and allow us to add the two spectra. The result is shown in panel (c) of figure 4, which represents the Cu(0 0 1)-$p(2 \times 2)$S L_3VV Auger line shape measured with excellent statistics.

Note that, as a comparison, the APECS spectrum is much more resolved than the single one (continuous line in figure 4(c)). This is owed to the remarkable decrease of

Table 1. Experimental values of $2p_{1/2}$, $2p_{3/2}$ energies and Lorentzian line-widths (in eV) obtained with left and right analyzer.

Analyzer	Energy $2p_{1/2}$	FWHM $2p_{1/2}$	Energy $2p_{3/2}$	FWHM $2p_{3/2}$
Left	133.69 (0.02)	0.19 (0.05)	134.87 (0.02)	0.08 (0.02)
Right	133.69 (0.01)	0.16 (0.03)	134.83 (0.02)	0.05 (0.01)

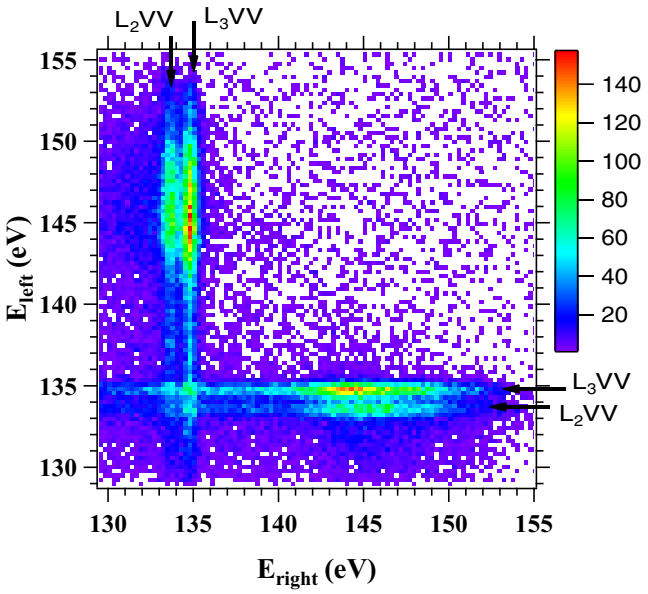

Figure 3. 2D true coincidence distribution. The black arrows indicate the coincidences due to LVV Auger electrons and $2p_{1/2}$ (L_2VV) and $2p_{3/2}$ (L_3VV) photoelectrons.

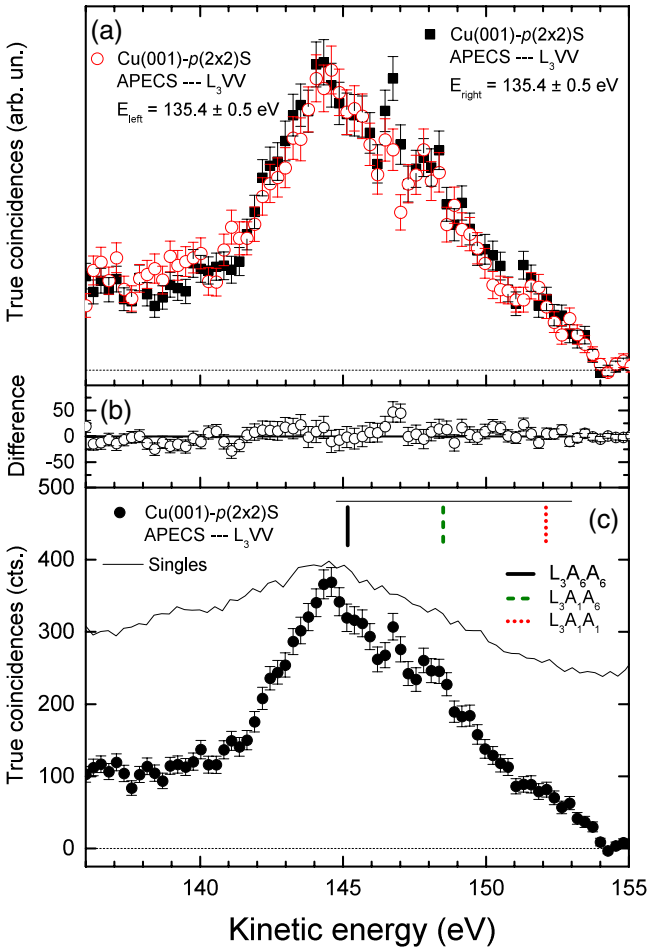

Figure 4. (*a*) S L_3VV Auger spectrum (in coincidence with $2p_{3/2}$ photoelectrons) measured with left (black squares) and right (red circles) analyzer. (*b*) Point by point difference of the curves shown in panel (*a*). (*c*) Cu(0 0 1)-$p(2 \times 2)$S L_3VV APECS spectrum obtained by summing the curves in panel (*a*). The bar plot shows the energies of the most intense transitions ending with two holes in S/Cu surface states. The continuous line represents the single Auger spectrum.

the background due to the fact that most of the secondary electrons have no time correlation with the photoelectron and do not contribute to the coincidence signal, beyond the already mentioned selection of a core-hole state which suppresses the contributions of other Auger decays. In addition, the increased surface sensitivity in the coincidence experiment [35–37] reduces the contributions of energy-loss events that are responsible for the low-energy tails in conventional Auger spectra.

The same analysis was performed for the Cu(0 0 1)-$p(2 \times 2)$S LVV Auger spectrum in coincidence with the $2p_{1/2}$ photoelectron. An accurate comparison of L_2VV and L_3VV spectra indicates that the two Auger transitions, though shifted in energy, display an identical line shape. This confirms the absence of Coster–Kronig preceded L_3(V)-(V)VV decays [21].

4. Discussion

The experimental results are now discussed in terms of a theoretical analysis of the CVV line shape. In an independent particle picture, the CVV spectrum is proportional to the self-convolution of the single particle density of occupied states, apart from matrix element effects and a shift corresponding to the core-hole energy. Hence, we start by analyzing the DOS projected on the sulfur atomic orbitals, as computed by DFT, which is shown in figure 5(*a*). The most important contribution has *p* symmetry around the nucleus (shaded, gray region), with the occupied portion having an overall width $W \approx 6$ eV. It is characterized by two peaks at -5 and -1 eV with respect to the Fermi level, E_F. These are usually labeled as A_6 and A_1, respectively [53]. Taking two non-interacting electrons within that band (see the $U = 0$ curve in figure 5(*b*)) it is possible to explain the main features observed in the L_3VV (L_2VV) spectrum. The linewidth of about 12 eV is twice the single-particle DOS width W. The three structures at about 145, 148.5 and 152 eV kinetic energy (indicated by vertical bars in figure 4(*c*)) correspond to transitions with two holes left in the A_6 (A_6A_6), one hole left in the A_1 and one in the A_6 (A_1A_6) and two holes left in the A_1 (A_1A_1) single particle

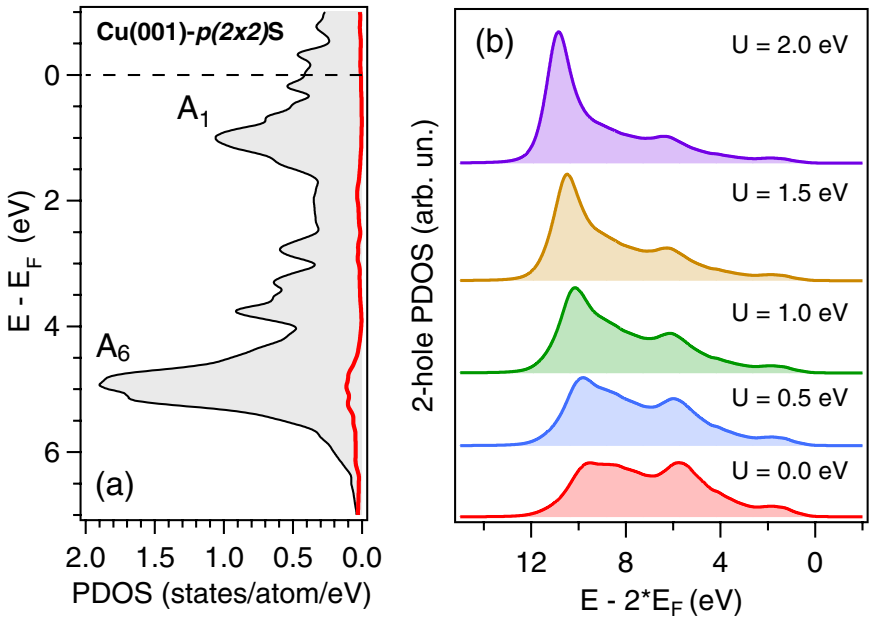

Figure 5. (*a*) DFT single-particle density of states projected on the atomic s (thick line) and p (shaded, gray area) orbitals of the sulfur atom. (*b*) Two-particle density of states for two holes at S/Cu surface states as evaluated by the Cini-Sawatzky theory, see (1), for different values of the hole–hole interaction energy, U.

states, respectively. We can conclude that in this system U is significantly smaller than W.

We now consider the effect of the hole–hole interaction within the CS theory and evaluate the two-particle interacting DOS in the atomic region by (1). It is interesting to address the dependence of the results on the value of U. This is shown in figure 5(*b*). As U increases, spectral weight is progressively transferred to more strongly bound states, thus enhancing the A_6A_6 peak as it is found in the experiment. Eventually, a split-off state (not shown) dominates the spectrum.

A quantitative analysis was then performed by fitting the line shape using the calculated two-particle DOS with different U values as trial functions and U as a fitting parameter. To account for the energy resolution of the experimental apparatus the theoretical functions were convoluted with a Gaussian profile of 0.8 eV full width at half maximum. The Auger spectrum is superimposed on a background, due to inelastically scattered electrons, whose intensity increases at lower kinetic energies. This background, reproduced by means of a Shirley-type function (dashed dotted line in figure 6), is summed to the theoretical results (yielding the solid and the dashed lines) to facilitate the comparison to experimental findings. The independent-particle approximation (dashed, green line) is able to explain the main features of the measured line. However, the self-convolution of the DOS is not able to reproduce the relative intensities of the main Auger transitions, due to the influence of the two-hole correlation energy in the valence band. Despite the two high kinetic energy transitions being very well characterized, the most intense A_6A_6 transition at 145 eV is underestimated.

The best fit between theory and experiment is then obtained with a relatively small amount of $U = 0.3 \pm 0.1$ eV (solid, red line). With such a value the relative intensities of the three main features associated to final states with two holes in the valence band are in excellent agreement with the measurements. Conversely, for $U > 0.4$ eV the spectral weight of the line is transferred to the A_6A_6 feature and the intensities of the A_1A_6 and A_1A_1 peaks are too low to depict the experimental data. This can be observed in the curve calculated

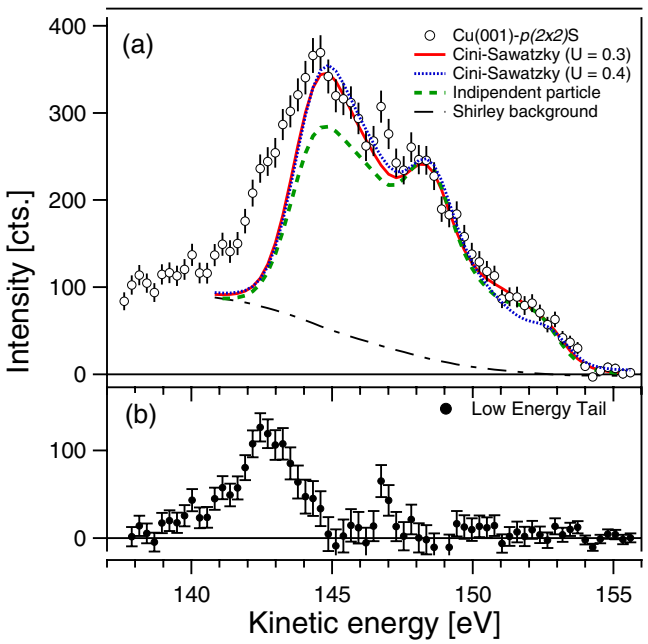

Figure 6. (*a*) Fits to the Cu(0 0 1)-$p(2 \times 2)$S L_3VV Auger line shape generated by the sum of a Shirley-type integral background (dashed dotted line) and the Cini-Sawatzky equation calculated for $U = 0.4$ eV (dotted line), for the best fit value of $U = 0.3$ eV (solid line) and for non-interacting particles ($U = 0.0$ eV) (dashed line). (*b*) Point by point difference of the coincidence data and the CS theory-calculated spectrum represented by the solid line in the upper panel.

for the upper limit value of $U = 0.4$ eV (dotted, blue line). Here, the data are still nicely reproduced but the intensity of the more energetic A_1A_1 peak is already underestimated.

A relatively high intensity of emission (∼20% of the total spectral weight) is observed in the low kinetic energy portion of the Auger spectrum. The characteristic energies of these emissions, $E_k \leqslant 143$ eV, are outside the energy range allowed by energy conservation in the CVV decay, corresponding to two holes at the bottom of the valence band. In order for Auger emission to be seen at these low energies, energy must have been transferred to some other excitation. These additional excitations could occur extrinsic to the core-hole decay, during the Auger electron transport throughout the specimen, or they could be an intrinsic part of the decay process. Previous APECS studies demonstrated that most of the low energy events in CVV Auger spectra of both wide band solids [61] and transition metals [62, 63] are not due to extrinsic losses but are an intrinsic part of the decay process.

Figure 6(*b*) shows the low energy tail (LET) of S L_3VV Auger spectrum obtained subtracting the CS spectrum calculated with $U = 0.3$ eV (solid line in figure 6(*a*)) to the coincidence data. Most of the LET intensity is included in a sharp feature at 142.5 eV. This presents a shoulder on the high kinetic energy side (∼144 eV) and a weak tail on the low kinetic energy one. The sharpness of the low energy transition with respect to the two-hole final state spectrum suggests that the latter is not the primary source of the observed LET. Indeed, with such a broad primary peak we would expect even the sharpest transitions to be smeared out.

The most likely picture is the one in which the generation of the additional electron–hole pair is intrinsic to the Auger process and due to valence band correlations. These kinds of processes are predicted to be particularly important for open shell systems, with a transition probability comparable to the one of two-hole final states [64]. As the process involves the excitation of one electron from the occupied to the unoccupied part of the valence band, the shape of the corresponding spectral feature essentially depends on the details of the valence states involved. The interaction among the three holes could be responsible for the localization of the final state of the process. Finally, the existence of such a feature is entirely dependent on the presence of correlation effects and this could be another hint of how the independent particle approximation cannot adequately describe the measured line shape.

5. Conclusions

In recent years, the study of Core-Valence–Valence (CVV) Auger decay has been demonstrated to be an established method to study the electronic properties in the valence band of a variety of systems. The nature of the Auger decay, in which one electron is removed from an ionized atom via an autoionization process, is such that it represents a prototypical process to determine the effects of electronic correlations in solids. These can be highlighted by comparing the measured Auger electrons' kinetic energy distribution with the one expected for non-interacting systems. In order to study correlation effects in Cu(0 0 1)-$p(2 \times 2)$S valence band we followed the aforementioned approach, with the peculiarity that the single-particle spectrum was obtained from DFT results. This allowed us to focus on the properties of the S atom which are most important given our interest in studying the surface states of the considered system.

We found that the main features of S L_2VV and L_3VV line shapes can be qualitatively understood within a single particle approximation, but a better description of the experimental data is obtained if a two-hole correlation energy of $U = 0.3 \pm 0.1$ eV is taken into account. A large part of the spectral weight (∼20%) occurs in an energy region forbidden by the two-hole CVV decay. The narrow shape of this low energy tail allowed us to associate it to the excitation of one additional electron–hole pair, as an intrinsic part of the core-hole decay.

Acknowledgments

We would like to thank the UE56/2-PGM2 beamline staff, in particular W Mahler and B Zada, for the valuable support provided during the experiment performed at the synchrotron-radiation facility BESSY II. This work was supported by the DFG via SFB 762.

References

[1] Lander J J 1953 *Phys. Rev.* **91** 1382–7
[2] Antonides E, Janse E C and Sawatzky G A 1977 *Phys. Rev.* B **15** 1669
[3] Cini M 1977 *Solid State Commun.* **24** 681–4
[4] Sawatzky G A 1977 *Phys. Rev. Lett.* **39** 504–7
[5] Hubbard J 1963 *Proc. R. Soc. Lond.* A **276** 238–57
[6] Cyrot M 1977 *Physica* B + C **91** 141–50
[7] Pickett W E, Erwin S C and Ethridge E C 1998 *Phys. Rev.* B **58** 1201–9
[8] Cococcioni M and de Gironcoli S 2005 *Phys. Rev.* B **71** 035105
[9] Himmetoglu B, Floris A, de Gironcoli S and Cococcioni M 2013 *Int. J. Quantum Chem.* **114** 14–49
[10] Kotliar G and Vollhardt D 2004 *Phys. Today* **57** 53–9
[11] Herring C 1966 *Magnetism* vol 4, ed G Rado and H Suhl (New York: Academic)
[12] Friedel J 1969 *Physics of Metals, I. Electrons* ed J Ziman (Cambridge: Cambridge University Press) p 340
[13] Lund C P, Thurgate S M and Wedding A B 1997 *Phys. Rev.* B **55** 5455–65
[14] Treglia G, Desjonqueres M C, Ducastelle F and Spanjaard D 1981 *J. Phys. C: Solid State Phys.* **14** 4347
[15] Bennett P A, Fuggle J C, Hillebrecht F U, Lenselink A and Sawatzky G A 1983 *Phys. Rev.* B **27** 2194–209
[16] de Boer D K G, Haas C and Sawatzky G A 1984 *J. Phys. F: Met. Phys.* **14** 2769
[17] Lof R W, van Veenendaal M A, Koopmans B, Jonkman H T and Sawatzky G A 1992 *Phys. Rev. Lett.* **68** 3924–7
[18] Gotter R, Bartynski R, Hulbert S, Wu X, Nozoye H and Zitnik M 1998 *J. Electron Spectrosc. Relat. Phenom.* **93** 201–7
[19] Arena D A, Bartynski R A, Nayak R A, Weiss A H and Hulbert S L 2001 *Phys. Rev.* B **63** 155102
[20] Butterfield M T, Bartynski R A and Hulbert S L 2002 *Phys. Rev.* B **66** 115115
[21] Haak H W, Sawatzky G A and Thomas T D 1978 *Phys. Rev. Lett.* **41** 1825–7
[22] Jensen E, Bartynski R A, Hulbert S L and Johnson E D 1992 *Rev. Sci. Instrum.* **63** 3013–26

[23] Sawatzky G A 1988 *Auger Electron Spectroscopy* vol 30, ed C L Briant and R P Messmer (Boston: Academic Press) pp 167–243
[24] Gotter R, Ruocco A, Morgante A, Cvetko L, Floreano L, Tommasini F and Stefani G 2001 *Nucl. Instrum. Methods Phys. Res.* A **467–8** 1468–72
[25] van Riessen G A and Thurgate S M 2006 *Surf. Interface Anal.* **38** 691–8
[26] Eland J H D, Vieuxmaire O, Kinugawa T, Lablanquie P, Hall R I and Penent F 2003 *Phys. Rev. Lett.* **90** 053003
[27] Hemmers O, Heiser F, Viefhaus J, Wieliczek K and Becker U 1999 *J. Phys. B: At. Mol. Opt. Phys.* **32** 3769
[28] Mase K, Kobayashi E and Isari K 2005 *Correlation Spectroscopy of Surfaces, Thin Films and Nanostructures* ed J Berakdar and J Kirschner (Weinheim: Wiley) pp 206–25
[29] Bartynski R A, Yang S, Hulbert S L, Kao C C, Weinert M and Zehner D M 1992 *Phys. Rev. Lett.* **68** 2247–50
[30] Stefani G *et al* 2004 *J. Electron Spectrosc. Relat. Phenom.* **141** 149–59
[31] Kakiuchi T, Hashimoto S, Fujita N, Tanaka M, Mase K and ichi Nagaoka S 2010 *Surf. Sci.* **604** L27–30
[32] Bartynski R A, Jensen E, Hulbert S L and Kao C C 1996 *Prog. Surf. Sci.* **53** 155–62
[33] Jensen E, Bartynski R A, Weinert M, Hulbert S L, Johnson E D and Garrett R F 1990 *Phys. Rev.* B **41** 12468–72
[34] Arena D A, Bartynski R A and Hulbert S L 2000 *Rev. Sci. Instrum.* **71** 1781–7
[35] Werner W S M, Smekal W, Störi H, Winter H, Stefani G, Ruocco A, Offi F, Gotter R, Morgante A and Tommasini F 2005 *Phys. Rev. Lett.* **94** 038302
[36] Werner W S, Stri H and Winter H 2002 *Surf. Sci.* **518** L569–76
[37] Liscio A, Gotter R, Ruocco A, Iacobucci S, Danese A, Bartynski R and Stefani G 2004 *J. Electron Spectrosc. Relat. Phenom.* **137–140** 505–9 (*Proc. of the 9th Int. Conf. on Electronic Spectroscopy and Structure (Uppsala, Sweden, 30 June—4 July 2003)*)
[38] See A, Siu W K, Bartynski R, Nangia A, Weiss A, Hulbert S, Wu X and Kao C C 1997 *Surf. Sci.* **383** L735–41
[39] Siu W K, Bartynski R A and Hulbert S L 2000 *J. Chem. Phys.* **113** 10697–702
[40] Sawhney K, Senf F, Scheer M, Schäfers F, Bahrdt J, Gaupp A and Gudat W 1997 *Nucl. Instrum. Methods Phys. Res.* A **390** 395–402
[41] van Riessen G, Wei Z, Dhaka R S, Winkler C, Schumann F O and Kirschner J 2010 *J. Phys.: Condens. Matter* **22** 092201
[42] Schumann F O, Dhaka R S, van Riessen G A, Wei Z and Kirschner J 2011 *Phys. Rev.* B **84** 125106
[43] Stefani G, Avaldi L and Camilloni R 1994 *New Directions in Research with Third-Generation Soft X-Ray Synchrotron Radiation Sources* (*NATO ASI Series* vol 254) ed A S Schlachter and F J Wuilleumier (Dordrecht: Springer) pp 161–88
[44] Perry D and Taylor J 1986 *J. Mater. Sci. Lett.* **5** 384–6
[45] Deroubaix G and Marcus P 1992 *Surf. Interface Anal.* **18** 39–46
[46] Mullins D, Huntley D and Overbury S 1995 *Surf. Sci.* **323** L287–92
[47] Colaianni M L and Chorkendorff I 1994 *Phys. Rev.* B **50** 8798–806
[48] Vlieg E, Robinson I K and McGrath R 1990 *Phys. Rev.* B **41** 7896–8
[49] Zeng H C, McFarlane R A and Mitchell K A R 1989 *Phys. Rev.* B **39** 8000–2
[50] Schach von Wittenau A E, Hussain Z, Wang L Q, Huang Z Q, Ji Z G and Shirley D A 1992 *Phys. Rev.* B **45** 13614–23
[51] Perdew J P, Burke K and Ernzerhof M 1996 *Phys. Rev. Lett.* **77** 3865–8
[52] Giannozzi P *et al* 2009 *J. Phys.: Condens. Matter* **21** 395502
[53] Monachesi P, Chiodo L and Del Sole R 2004 *Phys. Rev.* B **69** 165404
[54] Cini M and Verdozzi C 1989 *J. Phys.: Condens. Matter* **1** 7457
[55] Marini A and Cini M 1999 *Phys. Rev.* B **60** 11391–403
[56] Ma Y, Rudolf P, Chaban E E, Chen C T, Meigs G and Sette F 1990 *Phys. Rev.* B **41** 5424–7
[57] Schönhammer K and Gunnarsson O 1979 *Surf. Sci.* **89** 575–87
[58] Gunnarsson O and Schönhammer K 1980 *Phys. Rev.* B **22** 3710–33
[59] Gunnarsson O and Schönhammer K 1981 *Phys. Rev. Lett.* **46** 859–61
[60] Gotter R, Da Pieve F, Offi F, Ruocco A, Verdini A, Yao H, Bartynski R and Stefani G 2009 *Phys. Rev.* B **79** 075108
[61] Jensen E, Bartynski R A, Garrett R F, Hulbert S L, Johnson E D and Kao C C 1992 *Phys. Rev.* B **45** 13636–41
[62] Lund C P, Thurgate S M and Wedding A B 1994 *Phys. Rev.* B **49** 11352–7
[63] Mårtensson N, Nyholm R and Johansson B 1984 *Phys. Rev.* B **30** 2245–8
[64] Sarma D D and Mahadevan P 1998 *Phys. Rev. Lett.* **81** 1658–61